Photorefractive oscillators that use internal-reflection modes

Z. Ljuboje

Faculty of Electrotechnics, 71216 Lukavica, R. Srpska, Bosnia and Hercegovina

M. Belić

Institute of Physics, P.O. Box 57, 11001 Belgrade, Yugoslavia

D. Vujić

Faculty of Sciences, University of Kragujevac, P.O. Box 60, 34000 Kragujevac, Yugoslavia

F. Kaiser

Institute of Applied Physics, Darmstadt University of Technology, Hochschulstrasse 4a, 64289 Darmstadt, Germany

Received December 22, 1999; revised manuscript received July 18, 2000

Using the grating-action method, we analyze the operation of photorefractive oscillators that use internal-reflection modes of the crystal. We show that the oscillators interacting with the lossless internal modes possess no thresholds for coupling strengths and require no finite input seed for stable operation. The onset of oscillation is like a second-order phase transition, in contrast to the lossy oscillators, whose onset is like a first-order phase transition. © 2000 Optical Society of America [S0740-3224(00)01611-8]

OCIS codes: 190.4380, 190.5330.

1. INTRODUCTION

In a remarkable paper,[1] Lambelet, Salathé, Garrett, and Rytz analyzed a photorefractive phase conjugator by optical low-coherence reflectometry. The arrangement of rays and diffraction gratings within the $BaTiO_3$ crystal is reproduced in Fig. 1. It is the so-called cat arrangement, with an additional feedback loop coming from the opposite crystal corner. The paper[1] is interesting for a number of reasons[2]; however, we address only a particular aspect of it: Why is such an arrangement advantageous over the conventional cat geometry? Although it is alluded to in the paper that this geometry "should decrease the threshold for self-pumped phase conjugation," we show that indeed the phase conjugators in which the input beams interact with the lossless internal-reflection modes (IRM's) of the crystal possess no thresholds and require no input seeds for oscillation. In this sense these conjugators are the true self-pumped phase-conjugate mirrors.

A sample of such conjugators and modes is presented in Fig. 2. IRM's connect different corners in a principal cross section of a rectangular crystal. Even though IRM's are always of finite width, they can be very narrow. Some beautiful examples of photorefractive conjugators interacting with IRM's are given by Nowak, Moore, and Fisher.[3] We call these conjugators conserved, since the part of energy that is normally lost in a four-wave mixing (4WM) process is returned to the wave interaction region by IRM.

Conventional cat geometry has been the subject of intense interest since the days it was invented.[4] Even though it is easy to produce, understanding its operation is difficult. Even simple information, such as the threshold of operation, was subject to controversy. MacDonald and Feinberg[5] found that the threshold coupling strength (coupling constant times the thickness of the wave-mixing region) should equal 2.34, Cronin-Golomb *et al.*[6] found that it should be 4.68, and Belić *et al.*[7] found that it is 6.04. Here we show that it may actually vary continuously from 0 to ∞, depending on the transmissivity of the corner loop. In this manner the discussion of the exact threshold of the cat conjugator is found pointless.

The paper is divided into four sections. Section 2 introduces the method, Section 3 contains the analysis, and Section 4 offers some conclusions.

2. METHOD

We employ the grating-action method,[7] according to which the output slowly varying envelopes of the mixing waves in a 4WM process are given in terms of the input envelopes and one real quantity, the grating action u:

$$\begin{bmatrix} A_{1d} \\ A_{4d} \end{bmatrix} = \mathcal{T}(u) \begin{bmatrix} A_{10} \\ A_{40} \end{bmatrix}, \qquad \begin{bmatrix} A_{30} \\ A_{20} \end{bmatrix} = \mathcal{T}(u) \begin{bmatrix} A_{3d} \\ A_{2d} \end{bmatrix}, \tag{1}$$

where

$$\mathcal{T}(u) = \begin{bmatrix} \cos u & \sin u \\ -\sin u & \cos u \end{bmatrix}, \tag{2}$$

 © 2000 Optical Society of America

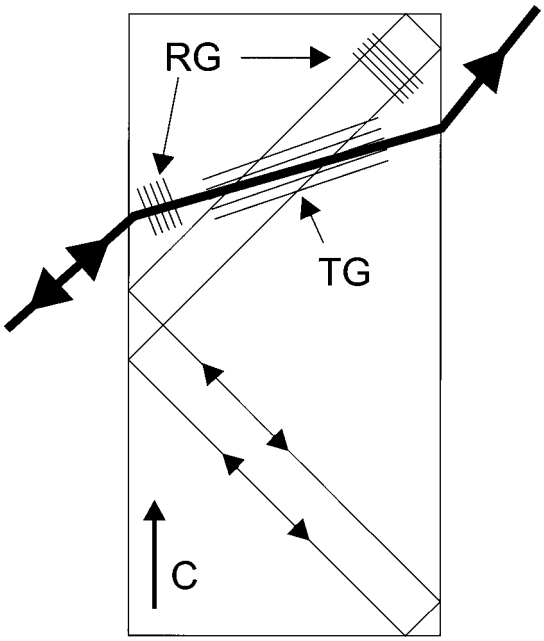

Fig. 1. Conserved cat conjugator, interacting with an internal-reflection mode. TG and RG stand for the transmission and the reflection gratings.

and the subscripts 0 and d denote the entrance and the exit face of the 4WM interaction region. The grating action u is calculated from the formula

$$\tan u = \frac{(A_{10}\bar{A}_{40} + \bar{A}_{2d}A_{3d} + \text{c.c.})}{I_{10} - I_{2d} + I_{3d} - I_{40} + aI_0 \coth(a\gamma/2)}, \quad (3)$$

where I_0 is the total intensity and γ stands for the coupling strength of the process. The bars denote complex conjugation. Only transmission gratings (TG's) are considered, even though it presents no difficulty to extend the discussion to the reflection gratings.[8] Steady-state, plane-wave, and degenerate conditions are assumed. Physically, ud represents an addition to the optical path in the crystal, owing to the formation of gratings.[8] a is a constant, to be found from

$$a^2 = \frac{P^2 + 4|Q|^2}{I_0^2}, \quad (4)$$

where $P = I_1 + I_2 - I_3 - I_4$ and $Q = A_1\bar{A}_4 + \bar{A}_2A_3$ is the amplitude of the grating.

In practical situations, Eqs. (3) and (4) should be applied to each of the 4WM regions comprising the oscillator, keeping track of all beams. This leads to a system of nonlinear algebraic equations, to be solved simultaneously for u and a values. In simple oscillators, such as the mutually incoherent beam coupler[9] (MIBC) or cat,[10] this leads to a system of four simple equations. However, in conserved conjugators, as described below, the situation is more complicated.

3. ANALYSIS

The case in question is the cat conjugator. It has been investigated thoroughly elsewhere,[5–7] from different points of view. Among other things, in the steady state, different thresholds are found for the onset of oscillation and different coupling strengths are found in the two regions. The analysis of the conserved cat adds another twist.

The geometry of Fig. 1 is presented again in Fig. 3(a), without reflection gratings and with the notational convention. The single extended TG region is replaced by two distinct 4WM regions, to reflect the general physical situation. We should mention that the device with one TG region is actually not the cat, as is discussed below. The letters r and t stand for the transmissivities of the lower- and the upper-corner internal reflections, which, in principle, could be different from each other. They are very important parameters in our analysis and exert crucial influence on the device threshold. Their physical relevance is clear, since internal modes, as observed experimentally,[1,3] can be quite lossy.

Application of Eqs. (3) and (4) leads to the following relations:

$$a' \coth(a'\gamma'/2) - 1 = -2rtE(ZF\cos u' + rtE\sin^2 u')/W, \quad (5a)$$

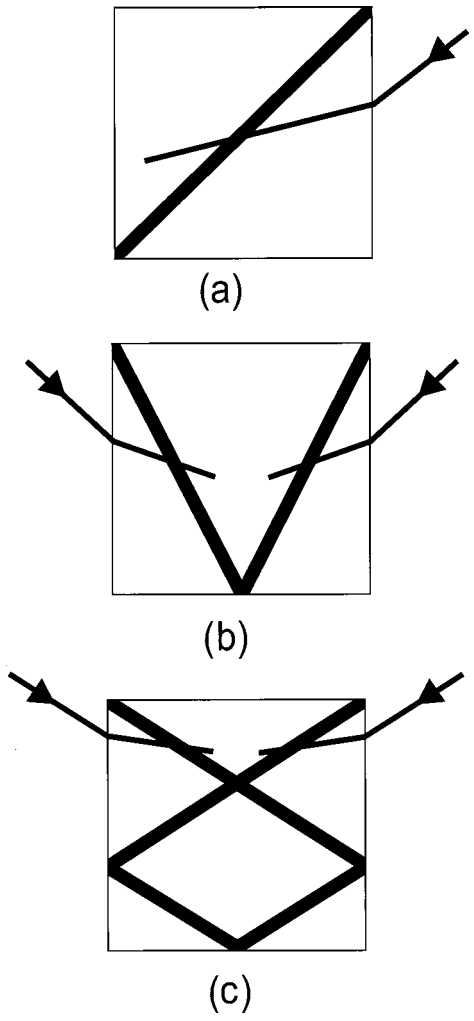

Fig. 2. Conserved conjugators that use the three basic internal-reflection modes (schematic): (a) degenerate mutually incoherent beam coupler, (b) bird-wing conjugator, and (c) frog-legs conjugator.

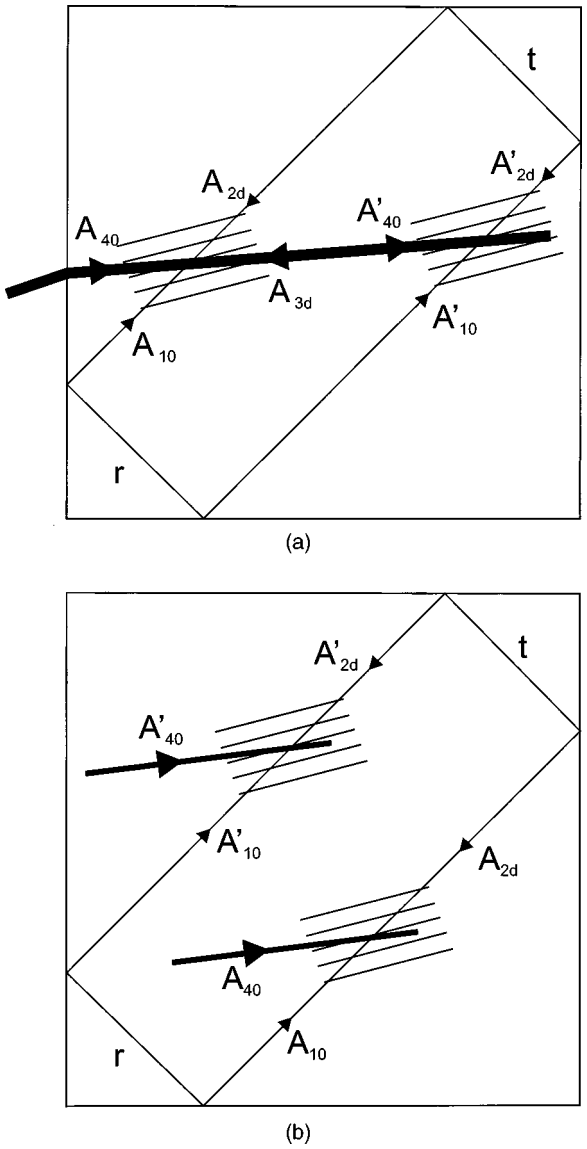

Fig. 3. (a) Conserved cat and (b) conserved mutually incoherent beam coupler. r and t denote the transmissivities of the lower and the upper portions of the internal-reflection mode.

$$1 - a'^2 = 4t^2Z^2 \sin^2 u(FZ \cos u' + rtE \sin^2 u')^2/W^2 \tag{5b}$$

for the primed region, and

$$a \coth(a\gamma/2) - 1 = Z[2t \cos u(Ht \sin^2 u' - Z^2 r \cos u') - Z \sin^2 u(1 + r^2t^2 \cos^2 u' + 2t^2 \sin^2 u') + Z(Z^2 - F^2)]/Y, \tag{5c}$$

$$1 - a^2 = 4t^2Z^2 \sin^2 u'(FH + Z \sin^2 u)^2/Y^2 \tag{5d}$$

for the unprimed region, where $E = rt \cos u' \cos u - \cos 2u$, $Z = rt \cos u' \cos u - 1$, $F = rt \cos u' - \cos u$, $W = r^2t^2E^2 \sin^2 u' + Z^2(t^2 \sin^2 u + F^2)$, $H = rt \cos u' \times (\sin^2 u + 1) - \cos u$, and $Y = Z^2(\sin^2 u + F^2) + t^2 \sin^2 u'(Z^2 \sin^2 u + H^2)$. The reflectivity of the device is given by

$$R = \frac{t^2(\sin u' \sin 2u - rt \sin u \, 2u')^2}{(rt \cos u' \cos u - 1)^4}. \tag{6}$$

These expressions are more complicated than the expressions for the conventional cat,[7] and the analysis is more involved. We assume that the same guiding principles govern the operation of the conserved cat as that of the conventional cat. The most important is Fermat's principle, which requires the operation of the device at the extremal value of the total optical action (including

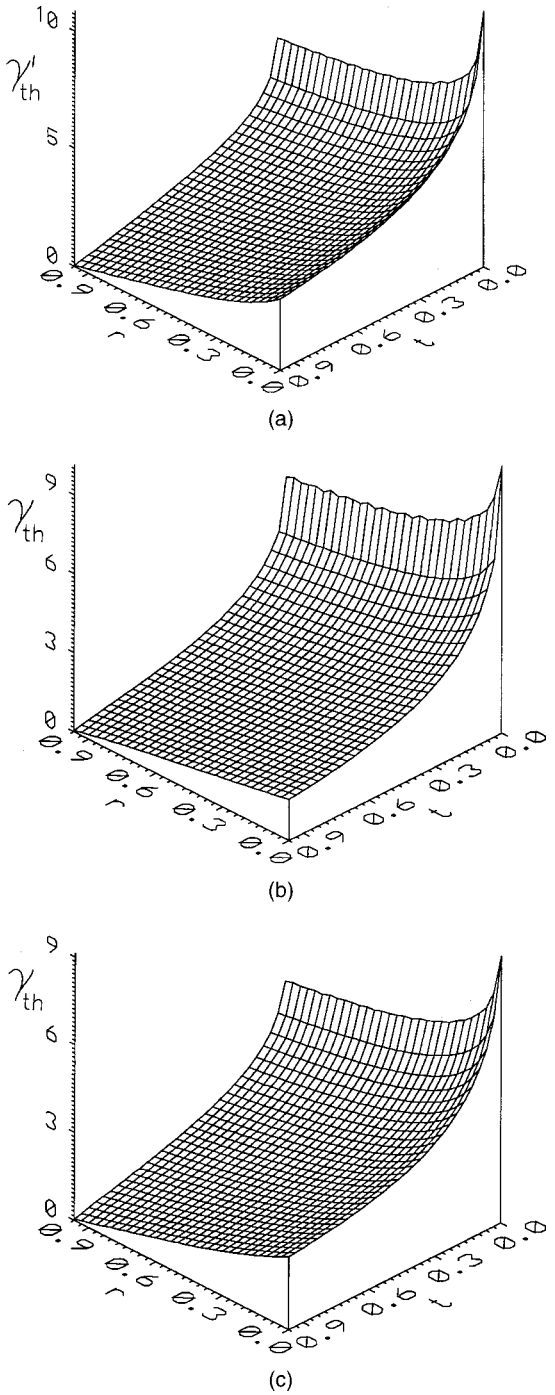

Fig. 4. Threshold surfaces of (a) the conserved cat, the primed region, (b) the conserved cat, the unprimed region, and (c) mutually incoherent beam coupler, one of the two (identical) regions, as functions of r and t. The last resolved value of t is 0.015.

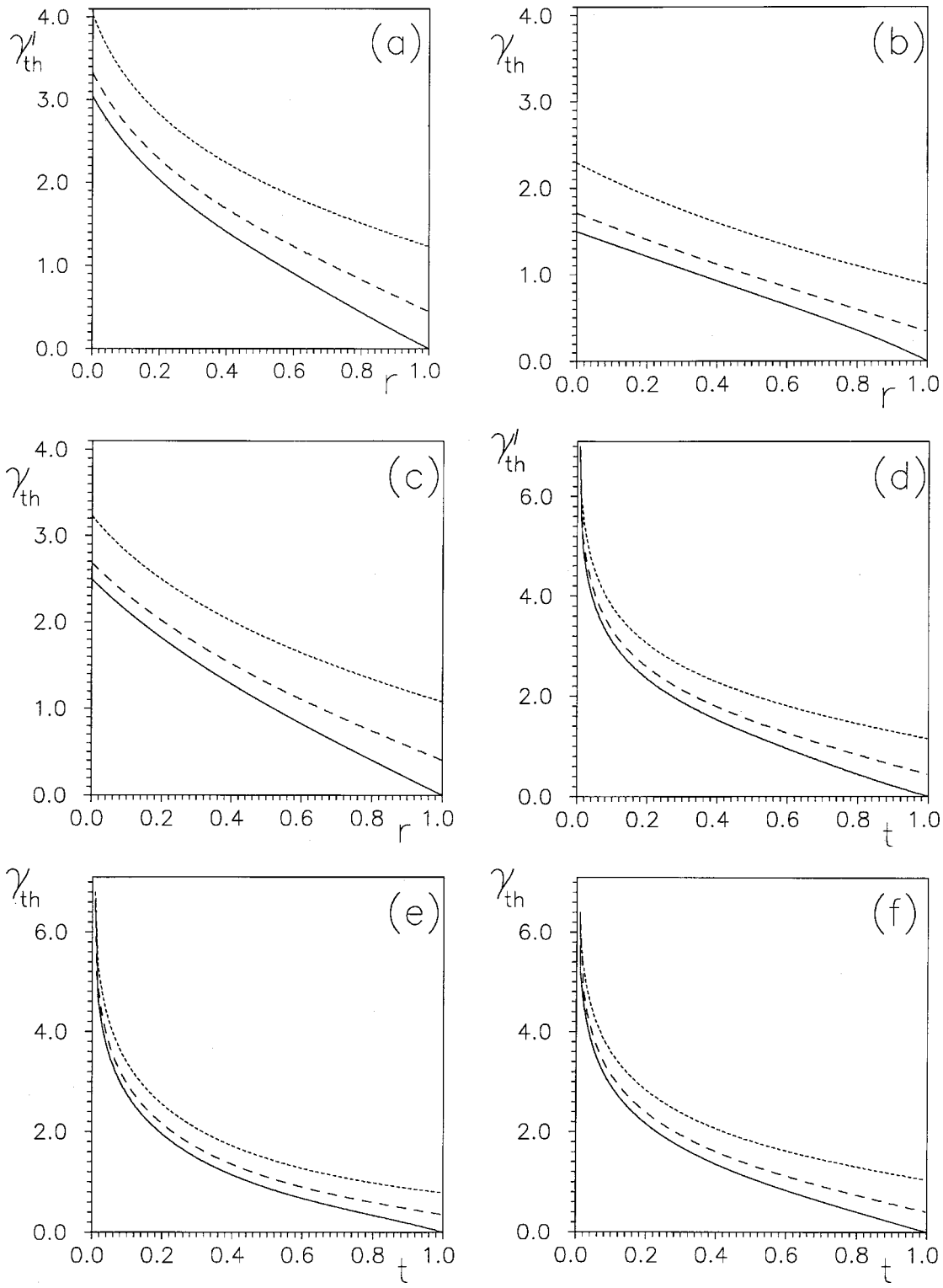

Fig. 5. Cuts through the three threshold surfaces from Figs. 4(a)–4(c). (a)–(c) Cuts parallel to the r axis for different values of t (solid curve, $t = 1$; dashed curve, $t = 0.8$; and dotted curve, $t = 0.5$). (d)–(f) Cuts parallel to the t axis, for the corresponding values of r.

the grating action). Fermat's principle governs the choice of both the threshold point and the operation point. The total grating action is $u' + 2u$, since the action of the primed interaction region is twice that of the unprimed region.[10,11]

The other guiding principle is equal participation of the two interaction regions at the threshold and operation points. There is no reason to assume that the regions contribute unequally to the operation of the device. This means $u' = 2u$, which greatly simplifies the analysis of Eqs. (5). The check on the analysis is the equivalence of results for the conventional and the conserved cat in the limit $r \to 0$. From the expression for R it is seen that the total grating action cannot be $u' + u$, and the equality

$u' = u$ cannot hold. For ideal feedback the reflectivity would always be zero.

The analysis is necessarily numerical, although in spirit it follows Ref. 7. Along the line $u' = 2u$ we determine the minimum value of a'_m in Eq. (5b), for some u'_m. Using the value of u'_m in Eq. (5d), we find the minimum values of a_m and u_m. Using these results in Eqs. (5a) and (5c), the threshold values of γ'_{th} and γ_{th} are calculated for the given values of r and t. The results are depicted in Figs. 4(a) and 4(b). A check on the procedure is that the values of $\gamma'_{\text{th}} \approx 3.04$ and $\gamma_{\text{th}} \approx 1.50$, found for the case $t \to 1$, $r \to 0$, are in agreement with the values for the conventional cat, obtained by different means.[7]

It is worth comparing the results for the conserved MIBC, whose geometry is presented in Fig. 3(b). Actually, the generalized MIBC interacting with the IRM should consist of four interaction regions and can be viewed as a system of two conserved cats. We consider the simplified version, with one 4WM region on each arm of the IRM, to be the proper extension of the conventional MIBC. This conjugator is unrelated to the conserved cat, which becomes obvious after the corresponding equations are written down:

$$a' \coth(a'\gamma'/2) - 1 = 2rtF \cos u/W, \tag{7a}$$

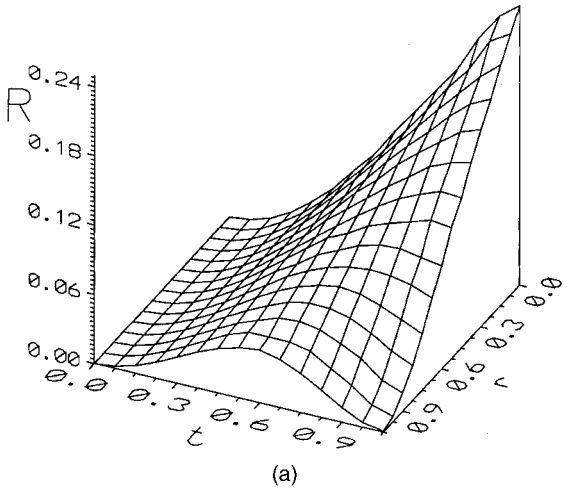

(a)

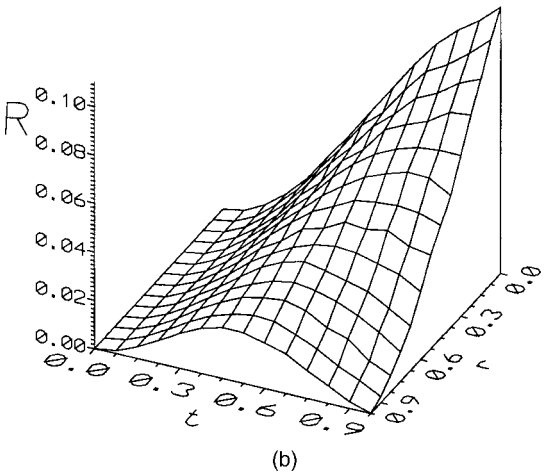

(b)

Fig. 6. Reflectivity surfaces at the threshold of (a) the conserved cat and (b) the mutually incoherent beam coupler, as functions of r and t.

$$1 - a'^2 = 4F^2q^2t^2 \sin^2 u/W^2, \tag{7b}$$

$$a \coth(a\gamma/2) - 1 = 2rtZ \cos u'/Y, \tag{7c}$$

$$1 - a^2 = 4t^2Z^2 \sin^2 u'/(q^2Y^2), \tag{7d}$$

where now $F = \cos u' - rt \cos u$, $W = F^2 + q^2t^2 \sin^2 u + \sin^2 u'$, $Z = \cos u - rt \cos u'$, and $Y = Z^2 + q^{-2}t^2 \sin^2 u' + \sin^2 u$. q^2 stands for the ratio of input intensities. The expressions for the reflectivity $R = I_{30}/I_{40}$ and the transmissivity $T = I'_{30}/I_{40}$ are given by

$$R = \frac{t^2 \sin^2 u \sin^2 u'}{q^2(rt \cos u \cos u' - 1)^2}, \tag{8a}$$

$$T = \frac{(\cos u - rt \cos u')^2}{(rt \cos u \cos u' - 1)^2}. \tag{8b}$$

These equations are different from the corresponding equations for the cat, even when $q = 1$. The two interaction regions in MIBC are identical to each other, whereas the two in the cat are not. The equations for MIBC are pairwise symmetric, whereas the equations for the cat are asymmetric. The operation of the two devices is different. MIBC can, and indeed prefers to, operate at equal grating actions $u' = u$, as then the reflectivity is maximized and the transmissivity is minimized. Nevertheless, the analysis of MIBC parallels that of the cat. Along the line $u' = u$ in Eqs. (7b) and (7d) one finds the minimum values of a'_m and a_m, for some u'_m and u_m. The consistency requires that $u'_m = u_m$, but in general $a'_m \neq a_m$. Only when $q = 1$ is it $a' = a$, and also $\gamma' = \gamma$. Upon substituting these values in Eqs. (7a) and (7c), one obtains the thresholds γ'_{th} and γ_{th}. The surface of γ_{th} for equal input intensities is shown in Fig. 4(c). The results are discussed in Section 4.

4. DISCUSSION

Interesting conclusions can be drawn. First, we consider the conserved cat. The dependence of the threshold on r, for a fixed t, is qualitatively similar to the dependence on t, for a fixed r. However, the threshold surface is not symmetric relative to the line $r = t$. The roles of the two transmissivities are different. This is clearly seen in Fig. 5. For example, for a fixed t and $r \to 0$, the conserved cat changes into a conventional cat. However, for a fixed r and $t \to 0$ the device does not function. The threshold blows up as $t \to 0$. In general, the smaller the transmissivities, the higher the threshold. It may vary from 0 to ∞, depending on the values of the IRM transmissivities. On the other hand, the threshold is zero as $r \to 1$, $t \to 1$. Then the device can operate at any nonzero values of the coupling strengths. Furthermore, the device reflectivity is zero at that point. The reflectivity surface at the threshold is displayed in Fig. 6(a). At the point $r \to 1$, $t \to 1$, no finite seeding is necessary for the start. The reflectivity grows smoothly as the coupling strength increases. The onset of oscillation for an ideal feedback is like a second-order phase transition. These conclusions are different from the conventional cat, which is not self-starting and has a high threshold. The reflectivity jumps discontinuously from zero to some finite value at

the threshold. The onset of oscillation in the conventional cat is like a first-order phase transition.

Similar conclusions hold for the conserved MIBC. We present only the case $q = 1$, for which it follows from the equations that $a' = a$ and $\gamma'_{\mathrm{th}} = \gamma_{\mathrm{th}}$. Hence only one γ_{th} is shown in Fig. 4(c). It approaches the value $\gamma_{\mathrm{th}} \approx 2.49$ of the conventional MIBC, as $t \to 1, r \to 0$. For ideal feedback the conserved MIBC possesses no threshold and starts to operate without the need for seeding, as can be seen in Fig. 6(b).

An interesting question is what happens to the conserved cat as IRM becomes narrow. Such modes, as well as the quasi-periodic ones (not closing on themselves) are allowed theoretically; however, in reality the 4WM regions fix the choice of the mode. For a narrow mode the two interaction regions overlap, and the internal optical path connecting them dissappears. The conserved cat collapses into the degenerate MIBC, i.e., the MIBC with one input beam. For this reason we denoted the device in Fig. 2(a) as the degenerate MIBC and not as the conserved cat. The rest of the conserved conjugators in Fig. 2 can be considered as two degenerate MIBC's interacting with the same IRM. The degenerate MIBC is described by Eqs. (7a) and (7b), in which $u = u'$ and $q = 1$. An experimental example is presented in Ref. 3.

In our understanding the cat will not interact with an IRM of narrow width because it requires two distinct interaction regions, which possess two different coupling strengths. It may happen that the two coupling strengths are equal, but it is more likely that they are not, since then the total grating action is lower and the reflectivity attained is higher. The authors of Ref. 1 placed only one TG region across both optical paths of the IRM in Fig. 1, presumably because they measured only one TG signal at the appropriate optical path depth. However, both TG regions of the conserved cat have the same optical path length, and their signals in the experimental setup of Ref. 1 would overlap. On the other hand, it is possible that the authors have observed the degenerate MIBC instead of the cat.

Many nice examples of cats interacting with broad internal-reflection rings, given in Ref. 3, are not of the kind described here. Those rings are unidirectional, and the interaction is through two-wave mixing, which is detrimental to the process of phase conjugation. Finally, it is worth mentioning that of all standard photorefractive oscillators, only the linear phase-conjugate mirror[6] is similar in operation to the conserved oscillators. It is self-starting, and the threshold is zero. However, it does not interact with the IRM, and the conserved operation is the consequence of choosing highly reflective external mirrors.

ACKNOWLEDGMENT

This work is supported by the Ministry of Science and Technology of the Republic of Serbia.

REFERENCES AND NOTES

1. R. Lambelet, R. P. Salathé, M. H. Garrett, and D. Rytz, "Characterization of a photorefractive phase conjugator by optical low-coherence reflectometry," Appl. Phys. Lett. **64**, 1079–1081 (1994).
2. Foremost for the skillful use of low-coherence reflectometry to identify and locate various gratings and their contributions to the PC signal along the entire optical path within the crystal.
3. A. V. Nowak, T. R. Moore, and R. A. Fisher, "Observations of internal beam production in barium titanate phase conjugators," J. Opt. Soc. Am. B **5**, 1864–1878 (1988).
4. J. Feinberg, "Self-pumped continuous-wave phase conjugator using internal reflections," Opt. Lett. **7**, 486–488 (1982).
5. K. R. MacDonald and J. Feinberg, "Theory of a self-pumped phase conjugator with two coupled interaction regions," J. Opt. Soc. Am. **73**, 548–553 (1983).
6. M. Cronin-Golomb, B. Fischer, J. O. White, and A. Yariv, "Theory and applications of four-wave mixing in photorefractive media," IEEE J. Quantum Electron. **QE-20**, 12–30 (1984).
7. M. Belić, M. Petrović, O. Sandfuchs, and F. Kaiser, "Threshold couplings of phase conjugate mirrors with two interaction regions," Opt. Lett. **23**, 340–342 (1998).
8. M. Belić and D. Vujić, "Interconnected ring oscillators," J. Opt. A (to be published).
9. A. M. C. Smouth and R. W. Eason, "Analysis of mutually incoherent beam coupling in $BaTiO_3$," Opt. Lett. **12**, 498–500 (1987).
10. M. Belić, M. Petrović, Z. Ljuboje, and F. Kaiser, "Threshold analysis of cat conjugator," Opt. Commun. **143**, 67–71 (1997).
11. M. Cronin-Golomb, "Almost all transmission gratings self-pumped phase conjugate mirrors are equivalent," Opt. Lett. **15**, 897–899 (1990).